Nanoelectrodes: Recent Advances and New Directions

Jonathan T. Cox and Bo Zhang

Department of Chemistry, University of Washington, Seattle, Washington 98195-1700; email: zhang@chem.washington.edu

Annu. Rev. Anal. Chem. 2012. 5:253–72

First published online as a Review in Advance on April 9, 2012

The *Annual Review of Analytical Chemistry* is online at anchem.annualreviews.org

This article's doi: 10.1146/annurev-anchem-062011-143124

1936-1327/12/0719-0253$20.00

Keywords

nanopore, voltammetry, electrochemistry, single nanoparticle

Abstract

This article reviews recent work involving the development and application of nanoelectrodes in electrochemistry and related areas. We first discuss common analytical methods for characterizing the size, shape, and quality of nanoelectrodes, including electron microscopy, steady-state cyclic voltammetry, scanning electrochemical microscopy, and surface modification. We then emphasize recent developments in fabrication techniques that have led to structurally well-defined nanoelectrodes. We highlight recent advances in the application of nanoelectrodes in important analytical chemistry areas, such as single-molecule studies, single-nanoparticle electrochemistry, and measurements of neurotransmitters from single neuronal cells.

1. INTRODUCTION

UME: ultramicroelectrode

SEM: scanning electron microscopy

TEM: transmission electron microscopy

The past three decades have seen tremendous growth and increased application of nanoelectrodes in fundamental electrochemistry, electrochemical analysis, electrocatalysis, and many other research areas. Nanoelectrodes typically refer to voltammetric electrodes with at least one dimension below 100 nm. They can be considered a special type of ultramicroelectrode (UME) with smaller critical dimensions. Most of the outstanding properties of UMEs, such as a small *RC* time constant and fast mass transfer, have been demonstrated on nanoelectrodes and are, in many cases, more pronounced. More than 20 years ago, Wightman (1) predicted, in one of his early papers on UMEs, some of the advantages of employing submicrometer electrodes. Penner et al. (2) stated that nanoelectrodes would find applications in various areas, such as neurophysiology, lithography, and chemical analysis. Since those important publications, research has progressed substantially in those areas.

Nanoelectrodes arose from the development of nanoband electrodes with bandwidths as small as 5 nm (3). Penner et al. (2) introduced glass-coated hemispherical nanoelectrodes that approached true molecular dimensions (~1 nm). Such nanoelectrodes offered many advantages because their geometric dimensions are smaller than the diffusion lengths normally encountered in other electrodes. The mass-transport rate increases as the electrode size decreases, and radial diffusion becomes dominant (4), which allows steady-state voltammetric responses to be readily achieved (1, 5). Other advantages include even smaller *RC* constants and the ability to make measurements in solutions of high resistance because of the lower influence of solution resistance (6).

In this review, we first discuss the analytical methods typically utilized to characterize nanoelectrodes. We then review recent advances in the fabrication of nanoelectrodes, highlighting some of the new methods reported in the literature. We also discuss challenges faced in the fabrication of structurally well-defined nanoelectrodes. In the last section, we review new applications of nanoelectrodes in electrochemical research. We emphasize the use of nanoelectrodes in studies of single nanoparticles and single redox molecules. We believe that there is great potential in taking advantage of the extremely small size of nanoelectrodes to make novel and useful measurements that cannot be achieved with macroscopic electrodes.

2. METHODS OF CHARACTERIZATION

It is vital to fully characterize the size and shape of a nanoelectrode because its electrochemical properties are often exceedingly sensitive to even small variations in its geometry. For example, the steady-state limiting current of a recessed nanoelectrode is smaller than that of a same-size disk nanoelectrode due to additional mass-transport resistance. Nanoelectrodes are typically characterized with electron microscopy, including scanning electron microscopy (SEM) and transmission electron microscopy (TEM), as well as various electrochemical methods. Unfortunately, it is often difficult to fully characterize a nanoelectrode with sufficient spatial resolution by use of electron microscopy, primarily because of charging effects from the insulation materials. Our laboratory is developing new nanoelectrodes to eliminate such problems. Electrochemical methods can provide a quick estimate of the size of a nanoelectrode on the basis of assumptions about its geometry. However, such results require microscopic verification.

2.1. Nanoelectrode Characterization by Electron Microscopy

Electron microscopy can be especially useful in obtaining quick and direct information about the shape and size of a nanoelectrode. The resulting information, however, is often limited by the

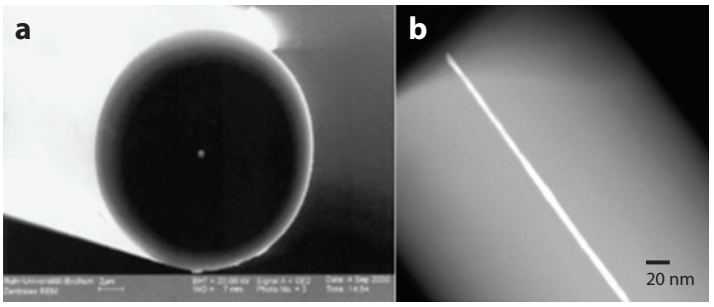

Figure 1

(*a*) A scanning electron microscope image of a 220-nm-radius disk Pt nanoelectrode. Reprinted with permission from Reference 19. Copyright 2002, Wiley. (*b*) A transmission electron microscope image of a 3-nm-radius Pt nanoelectrode encapsulated in quartz. Reprinted with permission from Reference 43. Copyright 2009, American Chemical Society.

spatial resolution of the instrumentation, the skill of the operator, and the sample properties of the nanoelectrode. SEM can reveal very useful three-dimensional information about a nanoelectrode's geometry. However, it has only limited spatial resolution with conventional tungsten-filament SEM. Field-emission SEM can provide enhanced spatial resolution on the order of 1 to 2 nm under optimized conditions, such as with the use of highly conductive samples. **Figure 1*a*** shows an SEM image of a quartz-encapsulated disk-shaped platinum (Pt) nanoelectrode with a radius of ~220 nm. Higher spatial resolution can be obtained by imaging nanoelectrodes with TEM. However, only certain nanoelectrodes with submicrometer overall dimensions can be imaged by TEM. **Figure 1*b*** shows a TEM image of a 3-nm-radius Pt nanoelectrode sealed in quartz. The high-energy electrons used in TEM can penetrate the thin silica insulating material, and the sub-10-nm Pt nanowire can be clearly resolved from the silica coating because of the z contrast between the nanowire and its environment.

2.2. Steady-State Voltammetry of Nanoelectrodes

Under conventional experimental conditions, the voltammetric response of a nanoelectrode can be characterized by a sigmoid-shaped steady-state voltammogram. Transient voltammetric responses can be obtained with sufficiently high sweep rates. For example, a 50-nm-radius nanoelectrode requires the sweep rate to be at least 1,000 V s^{-1} to show peak-shaped transient voltammetric behavior. Under this condition, the diffusion-layer thickness is estimated to be ~1 μm for a redox species with a diffusion coefficient of $\sim 10^{-5}$ cm^2 s^{-1}.

Figure 2*a* shows a steady-state cyclic voltammogram of an 86-nm-radius Pt nanoelectrode placed in acetonitrile containing 5 mM of ferrocene and 0.2 M of $TBAPF_6$ (tetra-*n*-butylammonium hexafluorophosphate). The oxidation of ferrocene at the surface of a nanoelectrode in solutions containing high concentrations of a supporting electrolyte is diffusion controlled, and the steady-state limiting current, i_{ss}, is easily observed. The magnitude of i_{ss} depends on the size and shape of the electrode. The general equation for i_{ss} is governed by the total mass-transfer resistance of the redox species from the bulk solution to the electrode (4):

$$i_{ss} = \frac{nFC_b}{R_{MT}}, \quad (1)$$

where n is the number of electrons transferred, F is Faraday's constant, C_b is the bulk concentration of redox species in solution, and R_{MT} is the mass-transfer resistance. For a disk-shaped

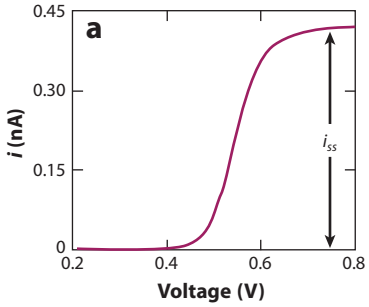

b Mass-transfer resistance to nanoelecrodes of different shapes

Band	Disk	Hemisphere
$\frac{\ln \frac{64Dt}{w^2}}{2\pi Dl}$	$\frac{1}{4Da}$	$\frac{1}{2\pi Da}$

Figure 2

(*a*) The steady-state voltammetric response of an 86-nm-radius Pt disk nanoelectrode. The radius of the electrode, *a*, is calculated from the magnitude of the steady-state limiting current, i_{ss}, and the mass-transfer resistance for a disk electrode geometry. (*b*) The equations for calculating the mass-transfer resistance of three different electrode shapes.

nanoelectrode such as the one used in **Figure 1*a***, the steady-state limiting current can be represented as follows:

$$i_{ss} = 4nFDC_b a, \quad (2)$$

where *a* is the radius of the disk nanoelectrode and *D* is the diffusion coefficient. The mass-transfer resistance varies for different electrode shapes (**Figure 2*b***). For a nanoband electrode, *l* and *w* represent the band length and the bandwidth, respectively. The time component, *t*, is equal to *RT*/F*v* (7), where *R* is the gas constant, *T* is the temperature, and *v* is the scan rate. Although the equation exhibits a slight time dependence, at long times the current–time relationship approaches a steady-state limiting current.

Steady-state cyclic voltammetry (CV) has several advantages that make it extremely useful for studies involving the use of nanoelectrodes. A steady-state cyclic voltammogram can be utilized to quickly evaluate the size of a nanoelectrode from the diffusion-limited steady-state current if one assumes the electrode is of a particular shape, such as a hemispherical electrode. Conversely, the limiting current can easily be employed to analyze the concentration of redox species by using nanoelectrodes of known size and shape. The shape of the voltammogram can be analyzed to provide useful information to evaluate the kinetics of heterogeneous electron transfer at the nanoelectrode surface (8, 9). By use of nanoelectrodes of specially designed geometry, such as nanopore electrodes, steady-state voltammetry can be utilized to study the transport of redox species in nanoscale spaces (10).

2.3. Nanoelectrode Characterization by Scanning Electrochemical Microscopy

Although the apparent size of a nanoelectrode can be readily extracted from steady-state CV, little or no information can be obtained about the shape of the electrode. Bard's group (8) was the first to use scanning electrochemical microscopy (SECM) to characterize nanoelectrode tips. In this method, an approach curve is generated as a nanoelectrode is lowered toward an insulating or conductive substrate in a solution containing an electroactive species. A potential is applied at the tip to induce the desired electrochemical reaction, and the current is monitored as a function of the distance from the substrate as the probe gradually approaches it. When the tip is far from the substrate, the measured current is the same as i_{ss}, and the radius of the electrode can be calculated from Equation 1. As the tip approaches the substrate, the observed current change depends on

CV: cyclic voltammetry

SECM: scanning electrochemical microscopy

the distance to the substrate and its conductivity. For a useful approach curve to be obtained, the tip must be moved to within one or two tip radii from the substrate. Doing so is challenging for small (e.g., <20-nm) nanoelectrodes, whose useful approach-curve distance range is short (11). The shape of the approach curve is governed by mass transport at the tip; by comparing the shape of the experimental approach curves with those from theory, one can ascertain the geometry of the electrode (12, 13).

2.4. Surface Adsorption and Charging

A challenge that arises in research into nanoelectrodes is the correlation between the apparent electrode size and the actual microscopic area. Recent studies have employed underpotential deposition at metal electrodes to obtain the actual electrochemically active surface area (14, 15). This process is usually carried out by electrochemically depositing a single layer of copper (Cu) atoms on the surface of the electrode through the application of a potential slightly more positive than the Nernst potential for Cu (16). The Cu is then stripped from the surface by sweeping the potential, which produces a current peak. The amount of charge for the oxidation of Cu is used to obtain the actual microscopic area (17).

White and coworkers (18) used another method to estimate the microscopic surface area. This method measures the electrical charge associated with the oxidation of an adsorbed complex molecule, *bis*-(2,2′-bipyridine)-chloro-(4,4′-trimethylenedipyridine)-osmium(II), by fast-scan CV. This method has been successfully used to measure Pt nanoelectrodes as small as 70 nm in radius. After the complex is adsorbed on the electrode surface, one must perform fast-scan CV, especially in the case of nanoelectrodes, because of the small number of redox molecules involved in the analysis. This method is advantageous because it is not always practical to obtain SEM or TEM images of every electrode employed in laboratories.

3. DEVELOPMENT OF NANOELECTRODE-FABRICATION TECHNIQUES

Numerous methods have been employed to produce nanoelectrodes of various shapes. Representative methods include micropipette pulling technology (12, 19), partial insulation of an electrochemically sharpened metal wire or carbon fiber in photoresist (20), Teflon® (21), electrophoretic paint (18, 22–24), and glass (2, 25). For a detailed summary of the materials and methods previously employed in nanoelectrode fabrication, please refer to Arrigan (26) and Zoski (27). Despite enormous progress, the controllable fabrication of structurally well-defined nanoelectrodes and their characterization at high spatial resolution remain challenging for their successful application. We review recent progress in the fabrication of band-, disk-, hemispherical, and pore-shaped nanoelectrodes. We briefly describe the preparation of nanoelectrode arrays and ensembles fabricated by deposition or by micro- and nanofabrication techniques.

3.1. Nanoband Electrode Fabrication

The White and Wightman groups first reported the use of nanoelectrodes in electrochemical studies, which had nanoband geometries (3, 5). The critical dimension of a nanoband electrode is its width. The nanoband can be millimeters or even centimeters long, which leads to larger observed currents than for nanodisks, while maintaining properties of radial diffusion. The voltammetric response observed at a nanoband electrode can be approximated by semi-infinite diffusion to a hemicylindrical electrode. The current density at a nanoband is more uniform across the surface,

thereby reducing large charges at the edge of the electrode. An additional advantage is that the geometric surface area scales linearly with the critical dimension, resulting in an electrode that is nanoscopic in width but macroscopic in length.

FIB: focused ion-beam milling

Several similar methods have been used to fabricate nanoband electrodes. Nanoband electrodes are generally fabricated by depositing a thin metal film on a substrate, depositing an insulating layer on top that electrically isolates it, and exposing the end of the electrode. Wightman et al. (5) first reported nanoband electrodes made by sputtering gold (Au) or Pt on a glass microscope slide. The thickness of the films varied from 30 nm to 2,300 nm. The authors isolated the films by applying an epoxy on top of the metal and exposing the metal by mechanical polishing. White and coworkers (3, 28) reported a similar method in which Pt films were sputtered on a mica substrate. These authors chose mica as a substrate because of its molecularly smooth surface. The quality of the nanoband electrode is strongly related to the uniformity of the metal film. Au films have a tendency to delaminate, which leads to defects in the metal film. To overcome this challenge, Caston & McCarley (29) modified this method by evaporating an Au film on a silanized glass substrate. The purpose of the silane modification is to increase the uniformity of the Au film. By first modifying the glass, the authors obtained small-grained electrically conductive Au films that were as thin as 3 nm.

An alternative form of the nanoband electrode is the ring-shaped nanoelectrode, which is formed on a glass rod or the inside walls of a glass capillary. Ewing and coworkers (30) formed a ultrathin carbon nanoring electrode inside a pulled-glass micropipette. The carbon ring was created through hydrocarbon pyrolysis of methane inside pulled-quartz capillaries. Very small ring nanoelectrodes with an overall diameter of less than 1 μm have also been developed. MacFarlane & Wong (31) fabricated a ring-shaped nanoelectrode through deposition of Au or Pt thin films on a glass or epoxy rod, followed by insulation and exposure of the edges of the metal films. Macpherson et al. (32) used a similar technique to prepare ring-shaped nanoelectrodes with painted metal films (typical thickness: 0.1–0.5 μm) around the outer edge of a capillary, followed by an epoxy resin insulating sheath.

Lanyon & Arrigan (7) and Lanyon et al. (33) used focused ion-beam milling (FIB) to fabricate recessed nanoband electrodes. They created Pt nanoband electrodes through UV lithography and metal deposition onto an oxidized silicon wafer substrate. They then deposited a thin film of silicon nitride to form an insulating layer and used FIB to directly mill the silicon nitride passivation layer. With the Pt area exposed, recessed nanoband electrodes with widths of roughly 100 nm were readily fabricated. By exposing multiple Pt areas, one can also fabricate arrays of recessed nanoband electrodes. A challenge to this approach is that the recesses are not etched isotropically by FIB, so the walls of the trench are nonvertical and exhibit a wall angle of approximately 19°. Another limitation is that the width of the band is limited by the width of the beam from the FIB device and by the depth of the pore from the thickness of the insulating layer.

Our group (34) recently reported a new electrochemical etching method to improve the fabrication of recessed nanoband electrodes (or nanotrench electrodes). In this method, the trench is not formed through FIB; rather, the nanoband electrode is etched electrochemically. This process allows for the isotropic etching of Au and a well-defined trench. We can control the recess depth by the length of etching time, and the width of the band is governed by the initial amount of Au deposited on the glass substrate.

Penner and coworkers (35–36) and others (37) recently used a method termed lithographically patterned nanowire electrodeposition (LPNE) to prepare metal nanoelectrodes on solid support. The Penner group's method involves the preparation of a sacrificial nickel (Ni) nanoband electrode by optical lithography followed by electrochemical deposition on the Ni to form a metal nanowire. A technique known as nanoskiving is attracting particular interest for its potential use

in fabricating nanoelectrodes. In nanoskiving, a planar-patterned thin film is sectioned with an ultramicrotome (38, 39). With this method, nanowires can be fabricated out of different materials, and the geometry of the wires is readily controllable. The Whitesides group (40) recently created nanowires from different metals and semiconductors. Dawson et al. (41) recently fabricated a device that incorporates nanowires through nanoskiving. In this method, the authors incorporated Au nanowires into silicon chip substrates; the resulting nanoelectrodes were similar to nanoband electrodes due to the geometry of the exposed end of the nanowires.

3.2. Disk Nanoelectrode Fabrication

Over the past decade, investigators have made substantial progress in the fabrication of disk nanoelectrodes. Many consist of glass-encapsulated metal nanoelectrodes in which a metal wire is sealed in an insulating sheath; a disk-shaped cross section results from exposing the end of the wire. The geometric area of a nanodisk electrode scales with the square of the radius, which can be made as small as a few square nanometers. Electrodes of such dimensions can be advantageous when one wants to examine faradaic reactions over a small area or to probe single redox molecules or nanoparticles. However, such small electrodes can result in measured currents that are quite small, and in some cases the detection of such small currents may be limited by instrumentation.

Nanodisk electrodes evolved from sharp-tip electrodes that were employed primarily for SECM (8) and neuroscience applications (42). Investigators refined these existing methodologies, which led to the fabrication of needle-type Pt disk electrodes via a laser-assisted pulling process first demonstrated by Shao et al. (12); this process was further improved by Katemann & Schuhmann (19). Our laboratory recently modified this procedure to fabricate Pt disk electrodes ranging in size from 1 to 3 nm (43). In this procedure, an ~25-μm Pt microwire is inserted into a thick-walled quartz capillary. This Pt microwire is sealed inside the capillary through laser heating and an in-house vacuum. After a complete seal is obtained, a pulling force is applied to the capillary, which draws the encapsulated Pt microwire into two ultrasharp tips. The diameter of the wire at the end of these tips can be well controlled in a range from ~2 to 10 nm. The end of the Pt wire is enclosed in a sheath of glass and exposed by mechanical polishing (13, 44). Because the tip is so small and fragile, one can employ an alternative to beveling, namely sealing the entire sharp tip in a borosilicate glass capillary before exposing the wire. After sealing, the wire is exposed through the use of fine sandpaper and an alumina suspension on a polishing cloth. The size of the exposed Pt disk electrode varies with the size of the initial Pt wire. If a smaller Pt wire is used, one can obtain a smaller Pt nanodisk electrode (43).

Rather than pulling, one can seal and expose sharp metal tips prepared through electrochemical etching (25). In this method, a Pt/Au microwire is electrochemically etched to a sharp tip in a NaCN/NaOH solution. The sharpened tip is then sealed into a piece of glass capillary and exposed to form a nanodisk through mechanical polishing. In both this method and the one described above, a major factor that affects the diameter of the disk is the amount of polishing.

Although Pt nanoelectrodes are regularly fabricated with the pulling method, difficulties arise when a different metal is used. Because the melting point of quartz glass (~1,670°C) is close to but below the melting point of Pt metal (~1,770°C), Pt wires can be readily pulled via the method mentioned above. In the case of Au, whose melting point is substantially lower (~1,060°C), it is more difficult to fabricate nanoelectrodes. As a result, the preparation of Au nanoelectrodes with laser pulling can be challenging. Mirkin and coworkers (45) have fabricated Au disk nanoelectrodes with radii as small as ~40 nm by using borosilicate glass.

Another way to fabricate small Au disk nanoelectrodes involves the electrochemical deposition of Au into Pt nanopore electrodes (46). This process is accomplished by first fabricating a Pt disk

nanoelectrode of the desired dimensions, then electrochemically etching the Pt to form a nanopore electrode (47). In the next step, the Au is electrochemically reduced inside the nanopore to form a nanowire. The excess Au is then polished away. As expected, the diameter of the Au nanoelectrode depends on the initial diameter of the Pt nanodisk electrode. This method has produced Au nanoelectrodes with radii as small as 4.5 nm (46). Despite recent progress in current fabrication methods for disk nanoelectrodes, challenges remain. A notable example is the agreement between geometric and effective electrochemical dimensions. Sun and coworkers (48) recently conducted a series of experiments showing the correlation of the geometric and electrochemical radii as determined by CV and SEM. They concluded that the geometric radius closely matches the effective radius when the electrode is greater than 20 nm. However, when the effective radius is less than 20 nm, the observed current fluctuates, probably because of potential fluctuations and double-layer effects. Also, the voltammetric behavior of nanoelectrodes differs from conventional voltammetric theory when the radius is below 10 nm (4, 49–51). A factor contributing to this phenomenon is that the current density on a disk is nonuniform and greater at the edge of the electrode. Another disadvantage of preparing nanoelectrodes of this manner involves leakage (14) and current fluctuation caused by a mismatch in expansion coefficients and by mechanical polishing. Following mechanical polishing of the electrode tips, it can be difficult to determine whether the exposed tip is planar or nonplanar; therefore, it is important to use SECM or other analytical methods to confirm the electrode's geometry.

3.3. Hemispherical Nanoelectrodes

The development of hemispherical nanoelectrodes arose from earlier work in producing tips for scanning tunneling microscopy (52, 53). Investigators usually fabricate such electrodes by coating an electrochemically etched metal or carbon microwire in an insulating material, then exposing the very end of the tip. Popular electrode materials include Au, Pt, and carbon fiber. Many coating materials have been utilized over the past 10 years, including glass (2, 54), wax (8), polymer (20), and electrophoretic paint (22–24). The size of the nanoelectrodes prepared through these methods can be affected by the sharpness of the tip and the quality of the insulating materials. Methods have been developed to further sharpen the electrochemically etched Pt or Au tips to achieve ultrasharp tips with a radius of apex below 5 nm (25). A disadvantage of these methods is that the size and the shape of the resulting nanoelectrodes are somewhat difficult to control.

3.4. Nanopore Electrodes

As a special type of nanoelectrode, nanopore electrodes have been the subject of tremendous research interest in the past decade (47). A nanopore electrode is a solid-state nanopore with an electrode created at the bottom that is utilized to monitor the flux of redox species through the nanopore orifice. Glass nanopore electrodes of both conical (47) and cylindrical shapes (44) have been reported. Nanopore electrodes are especially useful for studying molecular transport through solid-state nanopores. Wang et al. (10) have reported modification of glass nanopore electrodes with functional organosilanes to influence the transport of charged redox species. In addition, the extremely small volume inside the nanopore electrode can be utilized to study the electrochemical properties of trapped single redox molecules. For example, Sun & Mirkin (55) have reported single molecule–type experiments in nanopore electrodes with volumes as small as a zeptoliter. We have recently reported the preparation of metal nanoelectrodes by electrochemical deposition inside the nanopores of Pt nanopore electrodes (46).

The fabrication of a nanopore electrode can be easily accomplished through the electrochemical etching of a disk-shaped nanoelectrode to partially remove the electrode material. The

electrochemical etching of a Pt or Au nanoelectrode can be easily carried out in a NaCl solution with a small ac voltage signal (25). The size of the nanopore orifice is therefore limited by the size of the initial disk nanoelectrode. Glass-sealed disk nanoelectrodes have been extensively utilized to prepare glass nanopore electrodes. An interesting property of nanopore electrodes is that the faradaic current decreases as the depth of the nanopore increases, due to increased mass-transfer resistance (56). It is important to fully characterize the geometry of a nanopore electrode in order to use it in fundamental electrochemical studies and electrochemical sensing. The size of the nanopore orifice can be easily calculated from the steady-state voltammetric response of the initial disk nanoelectrode. Both steady-state CV and fast-scan voltammetry can be used to estimate the depth of the nanopore electrode. For a cone-shaped glass nanopore electrode, the angle of the cone can be measured optically by examining the conical metal tip prior to sealing it in glass. Although past research has focused mainly on the use of glass or quartz, other materials such as polymers can also be utilized to create nanopore electrodes with new functionalities.

SWNT: single-walled carbon nanotube

3.5. Carbon as a Nanoelectrode Material

Over the past decade, tremendous research efforts have been devoted to the use of carbon allotropes as materials for various electrochemical applications. The advantages of carbon as an electrode material for molecular electrochemistry include its low cost, inert electrochemistry, and wide potential window (57–59). Two specific areas that have attracted much recent attention are carbon nanotubes and graphene, both of which can be used as materials for nanoelectrodes with wide applications (60). Graphene is a carbon allotrope that consists of a single layer of carbon atoms with an arrangement similar to that of its multilayered counterpart, graphite (61). A carbon nanotube is essentially a graphene sheet that is rolled into a cylinder. The advantages of these materials arise from their well-ordered structure and relative ease of synthesis (62). These materials have potential applications in the field of molecular electronics; for a thorough review, see Reference 59. Graphene is beginning to attract attention as an interesting nanoelectrode material in preliminary studies using a graphene film as an electrode (63, 64) and in others highlighting its potential as an electrochemical sensor (65, 66). However, in this review, we focus on the use of single-walled carbon nanotubes (SWNTs) and carbon fibers as nanoelectrodes and their uses in analytical methods.

Crooks and coworkers (67) were among the first to use a multiwalled carbon nanotube as an electrochemical probe. Their reported nanoelectrodes consisted of carbon nanotubes, 80 nm to 200 nm in diameter, that had been electrically attached to sharpened Pt wires. The authors insulated the nanotubes by coating them with phenol, and they exposed the tip by applying a voltage to effectively cut the end of the tip and expose a fresh electrode. The observed sigmoidal voltammogram was characteristic of radial diffusion and similar to the response one would expect from a spherical nanoelectrode.

Individual SWNTs as nanoelectrodes were first reported by Dekker and colleagues (68, 69). In this method, a SWNT is grown through chemical vapor deposition onto a silicon wafer with a thermally grown oxide layer. The chip is coated with an SiO_x layer to insulate the SWNT. The surface of the SWNT is exposed through resist patterning by electron-beam lithography and hydrofluoric acid etching. The whole device is then coated with poly(methyl methacrylate) (PMMA) to electrically isolate the SWNT and prevent reactions from taking place on the titanium leads. A rectangular pit is patterned into the PMMA to expose the SWNT. This method is of particular interest because the SWNT can be either metallic or semiconducting in nature, according to the chirality of the nanotube. The side of the nanotube is exposed, and the electron transfer in each case can be individually studied. The Dekker group showed that there was no

significant difference in the electrochemical properties of either case. Macpherson and coworkers (70–73) used a similar method to fabricate electrodes composed of networks of SWNTs. In this method, multiple SWNTs are produced on an insulating surface via catalyzed chemical vapor deposition. This process creates a thin film of SWNTs that behaves similarly to a metallic film. This film can then be used as a substrate to deposit metal particles to form a network electrode. The authors have also used SECM to characterize the electrochemical behavior of SWNT network electrodes (73).

Carbon fiber microelectrodes have been extensively used in biological applications (74, 75). Most of the electrodes used in such studies are derivatives of carbon fibers that range from 5 to 10 μm. Huang et al. (76) showed that carbon fibers can be used to make nanoelectrodes by sealing a 7-μm carbon fiber inside a glass capillary and leaving one end of the fiber exposed. The exposed end is flame-etched by a low-temperature (~350°C) gas lamp. The resulting carbon fiber has a radius as low as 100 nm. A disadvantage of this method is that the resulting electrode is a wire protruding from a glass capillary, rather than an exposed disk. This type of electrode can be problematic because it can be difficult to fully characterize the electrode in sufficient detail.

3.6. Nanoelectrode Arrays and Ensembles

In this review, we focus primarily on individual nanoelectrodes rather than on nanoelectrode arrays or ensembles, but numerous nanofabrication methods can be used to produce arrays or ensembles of materials that are electrochemically active. In one of the first reported methods of this type, Menon & Martin (77) introduced nanoelectrode ensembles fabricated by the electroless deposition of Au in polycarbonate membranes. Other popular techniques include chemical etching (78, 79), lithography (80–83), nanoskiving (40), FIB (33, 84), and the use of networks of carbon nanotubes (70, 72, 85, 86). Nanoelectrode arrays and ensembles have wide applications in many analytical areas.

4. APPLICATIONS OF NANOELECTRODES

4.1. Fundamental Electrochemical Studies

The fast mass-transport rate of nanoelectrodes allows one to study the kinetic parameters of electrochemical reactions by using steady-state voltammetry (2, 11, 18, 43, 45). The kinetic parameters of nanoelectrodes are similar to those of microelectrodes. White and coworkers (18) showed the validity of these experiments by demonstrating that the electron-transfer rate is independent of mass transport to the electrode. Sun & Mirkin (11) advanced these studies by controlling the mass-transport rate using SECM in positive feedback mode and controlling the tip-to-substrate distance. The mass-transport rate changed on the basis of electrode size and geometry by as much as two orders of magnitude, with little effect on the heterogeneous rate constant. Further research revealed that the electron-transfer rate of outer-sphere reactions is also independent of electrode material (45). The Au nanoelectrodes employed in this study showed similar electrode kinetics as did Pt in the case of ferrocene, ferrocenemethanol, and tetrathiafulvalene. However, the reduction of hexaaminеruthenium(III) chloride at Au had a slightly lower rate.

In addition to kinetic parameters, the effects of the electrical double layer can also be extracted with nanoelectrodes. Using nanoelectrodes, White and coworkers (87, 88) and Chen & Kucernak (89) studied the effects of the double layer on mass transport by varying the ionic strength of solution. These studies suggest that nanoelectrodes may deviate from classical mass-transport models because the influence of interfacial electric fields on molecular transport is amplified as

electrode dimensions decrease. The effective electric field in this region may enhance or impede molecular transport, depending on the charge of the redox species. Another effect is the possible breakdown of electroneutrality at nanoelectrodes. Both of these effects cause the migration of redox molecules to play a significant role in mass transport to the electrode. These effects can be effectively studied by observing the steady-state voltammetric behavior. Recently, White and coworkers (88) investigated a conical nanopore electrode and its electrochemical behavior. The authors studied the diffusive and migrational flux of redox molecules through solid nanopores and demonstrated that the flux depends on the charge of the redox molecules and the relative concentration of the supporting electrolyte. Chen et al. (49–51, 90) have conducted similar research on the dynamic diffuse layer and deviations of nanoelectrodes from traditional voltammetric theory. Furthermore, numerical studies have analyzed the Poisson-Boltzmann equation for the electric field in an electrolytic solution adjacent to a charged surface (91). This experiment demonstrated that the diffuse double layer at a charged nanoelectrode differs significantly from the predictions made by classical Gouy-Chapman theory.

4.2. Single-Enzyme Electrochemistry

Lemay and coworkers (92) recently used protein film voltammetry to study the electrochemical behavior of a redox protein catalyst, [NiFe]-hydrogenase. In preliminary studies, these authors modified SWNT nanoelectrodes with the peptide polymyxin; they then immobilized an active submonolayer of [NiFe]-hydrogenase on an electrode substrate by using polymyxin and found that the adsorbed enzyme exhibited stable electrocatalytic behavior. This procedure was scaled down for use with lithographically fabricated Au nanoelectrodes to probe the catalytic behavior of a small number of enzyme molecules (93). The Lemay group measured the responses of an estimated 8 to 46 enzyme molecules. As Bard (94) discussed in his commentary on the Lemay group's publication, the expected response from a single enzyme would be ~1.6 fA, which is well below that of most state-of-the-art electrochemical instruments.

4.3. Single-Nanoparticle Electrochemistry and Electrocatalysis

The extremely small size of nanoelectrodes allows single nanoparticles to be studied. We (15, 46) and others (95) recently immobilized single metal nanoparticles on Pt and Au nanoelectrodes and studied their fundamental electrochemical properties and their size-dependent electrocatalytic activities (15). This is an important analytical strategy to learn the true size- and shape-dependent electrochemical and electrocatalytic properties of metal nanoparticles. Most current studies rely on the use of nanoparticle ensembles to understand the structure-dependent electrocatalytic properties of nanomaterials (96, 97). A challenge posed by using an ensemble is that only averaged properties can be derived. Additionally, the electrochemical results are especially sensitive to particle spacing (98) due to overlapping between diffusion layers, which is difficult to control in most cases. In our experiments, we directly examined the properties of single nanoparticles by connecting a single nanoparticle to a nanoelectrode. **Figure 3*a*** shows a schematic of a single-nanoparticle electrode (SNPE). The nanoelectrode surface is first modified by a linker molecule, either a silane or a thiol, and subsequently immersed in a solution of Au nanoparticles to form an SNPE. The radius of the disk electrode is smaller than that of the nanoparticle, so that, it is believed, only one particle chemically attaches to the surface. The SNPE can be characterized by CV and TEM to confirm the presence of the nanoparticle on the electrode. **Figure 3*b*** shows a TEM image of a single Au nanoparticle immobilized on a Pt nanoelectrode surface.

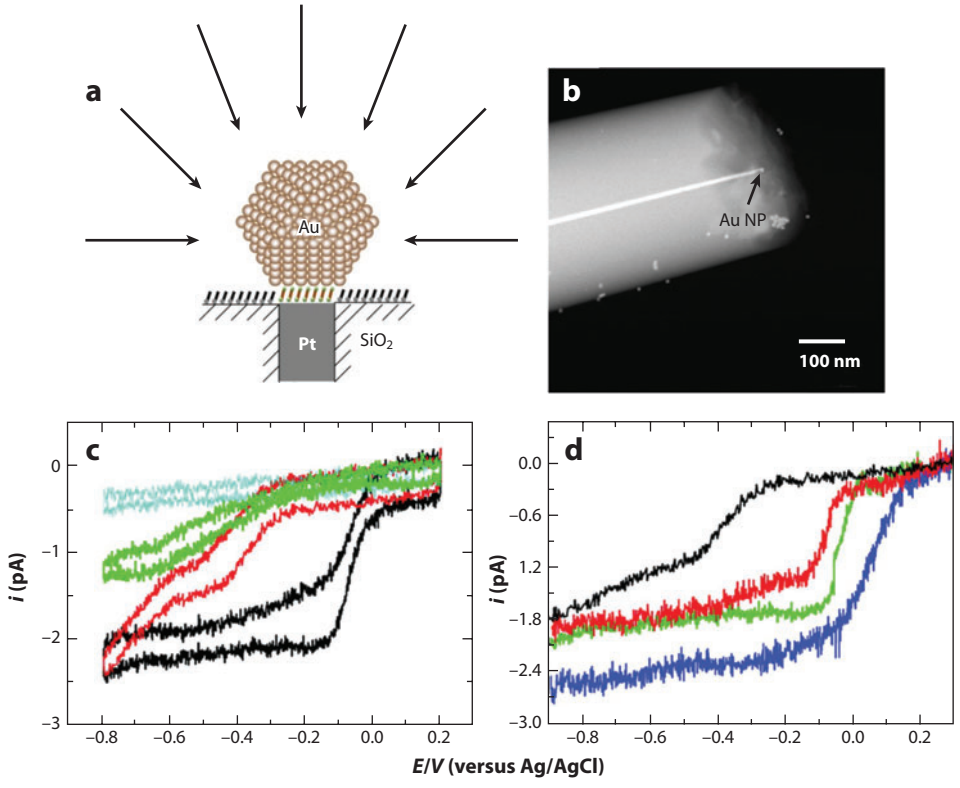

Figure 3

(*a*) Schematic of a single-nanoparticle Au electrode and the radial-type diffusion profile. (*b*) Transmission electron microscope image of a single Au nanoparticle (Au NP) immobilized on a Pt nanoelectrode. (*c*) Voltammetric responses in an O_2-saturated 0.10-M KOH solution of an 18-nm Au single-nanoparticle electrode (SNPE) (*black*), a 3-aminopropyltrimethoxysilane (APTMS)-modified Pt nanoelectrode (*green*), the bare Pt nanoelectrode (*red*), and an 18-nm Au SNPE after the nitrogen is bubbled (*cyan*). (*d*) Voltammetric responses in an O_2-saturated 0.10-M KOH solution of a bare 7-nm-diameter Pt nanoelectrode (*black*), a 14-nm Au SNPE (*red*), an 18-nm Au SNPE (*green*), and a 24-nm Au SNPE (*blue*). The scan rate was 10 mV s^{-1}. Reprinted with permission from Reference 15. Copyright, 2010 American Chemical Society.

Our initial studies revealed that the catalytic activity of Au nanoparticles toward the oxygen-reduction reaction (ORR) is size dependent. **Figure 3*c*** shows the current-voltage response of Pt nanoelectrodes and Au SNPEs of various sizes in a KOH solution used to probe the electrocatalytic response of Au nanoparticles toward ORR. The bare Pt nanoelectrode exhibits a two-step process for oxygen reduction. When a silane is attached to the Pt electrode, the half-wave potential for oxygen reduction shifts negatively, and the limiting current decreases significantly. Interestingly, the Au SNPEs exhibit a one-step process for oxygen reduction with an increased limiting current, compared with that of the bare Pt electrode. The half-wave potential for oxygen reduction is also shifted to −0.07 V, which suggests that, in this case, the Au SNPE demonstrates good electrocatalytic activity for oxygen reduction. **Figure 3*d*** compares the voltammetric responses of different-sized Au SNPEs and a bare Pt nanoelectrode. The steady-state limiting current increases, and the half-wave potential shifts to the right as the size of the nanoparticle increases,

which indicates greater catalytic activity. This result is interesting because we have observed size-dependent catalytic activities for Au nanoparticles even larger than 10 nm. Further insight into the catalytic properties of nanoparticles could be gained by utilizing nanoparticles of different shapes.

4.4. Stochastic Electrochemistry

Stochastic electrochemistry is the study of the faradaic current-voltage response associated with a random individual event measured on the surface of an electrode as a function of time, concentration, and electrode size, rather than a continuous current (99). This important method was recently used by Bard and coworkers (100–102) to study the electrochemical properties of single nanoparticles. In such experiments, metal or metal oxide nanoparticles colliding with an inert electrode surface are observed through electrochemical amplification by electrocatalysis. This method exploits the facts that the electrode itself is an inert substrate and that heterogeneous electron transfer of a given reaction occurs only when a nanoparticle comes into contact with the electrode. In the hope of increasing the signal-to-noise ratio, these authors recently extended their studies to the use of nanoelectrodes as an inert substrate. An example of such an experiment would be to use a Pt nanoelectrode with IrO_x nanoparticles in a 0.1-M NaOH solution. The reaction of interest, the oxidation of water, does not take place on the Pt nanoelectrode. It occurs only when an IrO_x nanoparticle comes into contact with the surface. The responses from the aforementioned experiment have been characterized through analysis of the frequency of events, the magnitude of the current of the events, and the shape of the current from the current-versus-time response. Such experiments yield critical information about size-, shape-, and structure-dependent catalytic activities (103).

4.5. Scanning Probe Techniques

SECM itself is a broad topic; extensive reviews have been written on the subject, showcasing various important applications (104, 105). Tip-based imaging techniques and nanoelectrodes have been integrated, and as fabrication methods improve, so will investigators' ability to study surface properties and local charge transport via SECM because one can obtain higher spatial resolutions with smaller electrodes (106). The Mirkin and Bard groups (8, 11, 12, 45) have conducted extensive research on the use of nanoelectrode probes in SECM. A focus of their research is the use of SECM to attain kinetic parameters, such as the heterogeneous electron-transfer rate, for various reactions.

SECM can be used in the substrate-generation/tip-collection mode to study reaction intermediates (107). This method uses the substrate to generate redox species and the tip for detection; it has been adapted by Mauzeroll and coworkers (108) to detect hydrogen peroxide as it is generated from a porphyrin monolayer by oxygen reduction. In this method, the substrate material is a thin film of porphyrin immobilized on a glassy carbon substrate, which reduces oxygen-generating H_2O_2. The H_2O_2 is detected by a Pt nanoelectrode tip. The use of a nanoelectrode probe allows local characterization of the substrate reactivity, which cannot be done with larger SECM probes. Etienne et al. (109) showed that SECM can be used in constant-distance mode to electrochemically measure the topography of a surface. The authors accomplished this task by using a conical and asymmetrical Pt tip to measure the current generated by the oxidation of hexaaminеruthenium(III) chloride at Au electrode surfaces at varying depths.

A method similar to SECM in the positive feedback mode involves the use of thin-layer cells constructed from nanoelectrodes to study electrochemical reactions in extremely small volumes

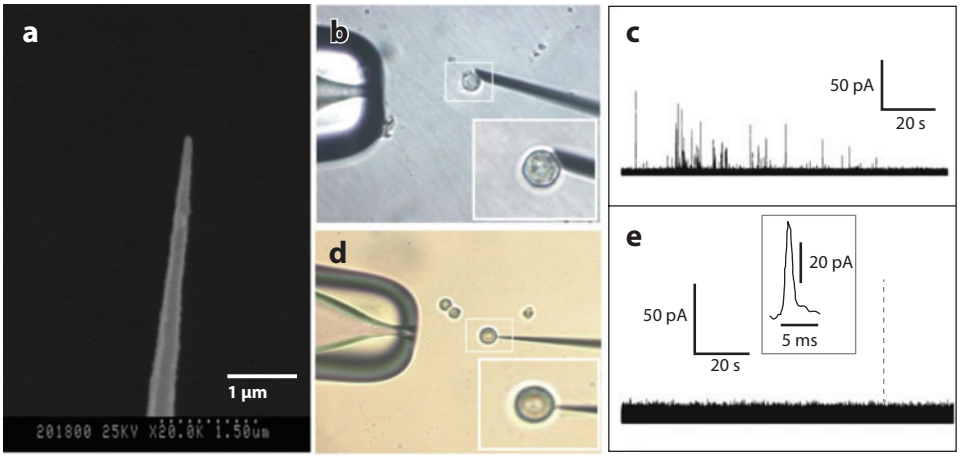

Figure 4

Monitoring of release from single PC12 cells by a microelectrode (diameter, 5 μm) and a nanoelectrode (tip diameter, ~100 nm). (*a*) Scanning electron microscope image of a nanoelectrode. (*b*,*d*) Photographs of actual microelectrode-cell and nanoelectrode-cell arrangements, respectively. (*c*) Results from a carbon fiber microelectrode. (*e*) Results from a nanoelectrode (diameter, ~100 nm). The current spikes are magnified in the inset. Reprinted with permission from Reference 113. Copyright 2005, American Chemical Society.

(44, 55). A thin-layer cell is constructed by electrochemical etching of a nanoelectrode, which forms a shallow nanopore electrode. This pore is filled with an aqueous solution and immersed in a mercury pool, producing a thin-layer cell with controllable dimensions. This method is similar to that first reported by the Bard group (110, 111), in which a molecule is trapped between a tip and a conductive substrate with a wax sheath, resulting in current amplification by the molecule being repeatedly oxidized and reduced between the two electrodes. Because of this effect and the small controllable volume, one can study the electrochemical reaction of a low number of molecules, even a single redox molecule.

4.6. Biological Applications

Exocytosis is an important biological process that has been widely investigated by scientists in various fields. One of the first major applications of UMEs was in the quantitative analysis of exocytosis. Wightman (1, 112) was the first to study neuronal secretion with carbon fiber microelectrodes. Recently, Wu et al. (113) utilized nanoelectrodes to study single-cell release by using amperometry. **Figure 4** shows an SEM image and photographs of cell arrangements of nanoelectrodes used in this study (113). When a planar UME is used to study a cell, the diameter of the electrode and that of the cell are similar. Due to their small size, nanoelectrodes can be used to study exocytotic events with significantly enhanced spatial resolution, which may allow researchers to effectively map exocytotic activities on a given cell. Wu et al. monitored the distribution of release sites and concluded that multiple vesicles can release dopamine at the same site. They have also conducted novel experiments combining capillary electrophoresis and nanoelectrodes to quantify dopamine from PC12 cells in a microfluidic device (114). Li et al. (115) have reported similar results. Such studies will provide us with additional insight into the process of exocytosis.

5. SUMMARY AND FUTURE DIRECTIONS

The development and application of nanoelectrodes in electrochemistry and many related areas have experienced enormous progress during the past decade. Because of their ultrasmall size, nanoelectrodes have numerous interesting properties that make them especially suitable for broad application in fundamental and applied studies in various fields. The development of new nanoelectrodes with well-defined structures and properties will continue to grow as new methods are developed, and especially as the use of nanofabrication techniques and facilities to fabricate nanoelectrodes increases. Such nanoelectrodes should allow precise correlation between the electrochemical properties and detailed structures of the electrode.

The study of single molecules and single nanoparticles is a new and important application of extremely small nanoelectrodes. This research area will benefit from new nanoelectrodes with submicrometer overall dimensions and well-defined structures to allow structural characterization with high-resolution electron microscopy. In addition, nanoelectrodes and their arrays will probably find extensive use in biological studies, such as imaging of subcellular structures and studies of transport properties of single ion-channel proteins on cells. Investigators will continue to obtain new and exciting information by using nanoelectrodes in fundamental studies.

DISCLOSURE STATEMENT

The authors are not aware of any affiliations, memberships, funding, or financial holdings that might be perceived as affecting the objectivity of this review.

ACKNOWLEDGMENTS

The authors gratefully acknowledge support from the Department of Chemistry at the University of Washington. The project or effort described was or is sponsored by the Department of Defense, Defense Threat Reduction Agency. The content of this review does not necessarily reflect the position or the policy of the federal government, and no official endorsement should be inferred. The authors thank past and present members of the Zhang research group and the departmental support staff for their hard work and commitment to excellence.

LITERATURE CITED

1. Wightman RM. 1981. Microvoltammetric electrodes. *Anal. Chem.* 53:1125–34A
2. Penner RM, Heben MJ, Longin TL, Lewis NS. 1990. Fabrication and use of nanometer-sized electrodes in electrochemistry. *Science* 250:1118–21
3. Morris RB, Franta DJ, White HS. 1987. Electrochemistry at Pt band electrodes of width approaching molecular dimensions—breakdown of transport equations at very small electrodes. *J. Phys. Chem.* 91:3559–64
4. Bard AJ, Faulkner LR. 2001. *Electrochemical Methods: Fundamentals and Applications*. New York: Wiley. 833 pp.
5. Wehmeyer KR, Deakin MR, Wightman RM. 1985. Electroanalytical properties of band electrodes of submicrometer width. *Anal. Chem.* 57:1913–16
6. Murray RW. 2008. Nanoelectrochemistry: metal nanoparticles, nanoelectrodes, and nanopores. *Chem. Rev.* 108:2688–720
7. Lanyon YH, Arrigan DWM. 2007. Recessed nanoband electrodes fabricated by focused ion beam milling. *Sens. Actuators B Chem.* 121:341–47
8. Mirkin MV, Fan F-RF, Bard AJ. 1992. Scanning electrochemical microscopy. 13. Evaluation of the tip shapes of nanometer size microelectrodes. *J. Electroanal. Chem.* 328:47–62

9. Watkins JJ, Zhang B, White HS. 2005. Electrochemistry at nanometer-scaled electrodes. *J. Chem. Educ.* 82:712–19
10. Wang GL, Zhang B, Wayment JR, Harris JM, White HS. 2006. Electrostatic-gated transport in chemically modified glass nanopore electrodes. *J. Am. Chem. Soc.* 128:7679–86
11. Sun P, Mirkin MV. 2006. Kinetics of electron-transfer reactions at nanoelectrodes. *Anal. Chem.* 78:6526–34
12. Shao YH, Mirkin MV, Fish G, Kokotov S, Palanker D, Lewis A. 1997. Nanometer-sized electrochemical sensors. *Anal. Chem.* 69:1627–34
13. Sun P, Mirkin MV. 2007. Scanning electrochemical microscopy with slightly recessed nanotips. *Anal. Chem.* 79:5809–16
14. Zhan DP, Velmurugan J, Mirkin MV. 2009. Adsorption/desorption of hydrogen on Pt nanoelectrodes: evidence of surface diffusion and spillover. *J. Am. Chem. Soc.* 131:14756–60
15. Li Y, Cox JT, Zhang B. 2010. Electrochemical responses and electrocatalysis at single Au nanoparticles. *J. Am. Chem. Soc.* 132:3047–54
16. Machado SAS, Tanaka AA, Gonzalez ER. 1991. Underpotential deposition of copper and its influence in the oxygen reduction on platinum. *Electrochim. Acta* 36:1325–31
17. Elliott JM, Birkin PR, Bartlett PN, Attard GS. 1999. Platinum microelectrodes with unique high surface areas. *Langmuir* 15:7411–15
18. Watkins JJ, Chen JY, White HS, Abruna HD, Maisonhaute E, Amatore C. 2003. Zeptomole voltammetric detection and electron-transfer rate measurements using platinum electrodes of nanometer dimensions. *Anal. Chem.* 75:3962–71
19. Katemann BB, Schuhmann T. 2002. Fabrication and characterization of needle-type Pt-disk nanoelectrodes. *Electroanalysis* 14:22–28
20. Sun P, Zhang ZQ, Guo JD, Shao YH. 2001. Fabrication of nanometer-sized electrodes and tips for scanning electrochemical microscopy. *Anal. Chem.* 73:5346–51
21. Liu B, Rolland JP, DeSimone JM, Bard AJ. 2005. Fabrication of ultramicroelectrodes using a "Teflon-like" coating material. *Anal. Chem.* 77:3013–17
22. Bach CE, Nichols RJ, Beckmann W, Meyer H, Schulte A, et al. 1993. Effective insulation of scanning tunneling microscopy tips for electrochemical studies using an electropainting method. *J. Electrochem. Soc.* 140:1281–84
23. Schulte A, Chow RH. 1996. A simple method for insulating carbon fiber microelectrodes using anodic electrophoretic deposition of paint. *Anal. Chem.* 68:3054–58
24. Slevin CJ, Gray NJ, Macpherson JV, Webb MA, Unwin PR. 1999. Fabrication and characterisation of nanometre-sized platinum electrodes for voltammetric analysis and imaging. *Electrochem. Commun.* 1:282–98
25. Zhang B, Galusha J, Shiozawa PG, Wang GL, Bergren AJ, et al. 2007. Bench-top method for fabricating glass-sealed nanodisk electrodes, glass nanopore electrodes, and glass nanopore membranes of controlled size. *Anal. Chem.* 79:4778–87
26. Arrigan DWM. 2004. Nanoelectrodes, nanoelectrode arrays and their applications. *Analyst* 129:1157–65
27. Zoski CG. 2002. Ultramicroelectrodes: design, fabrication, and characterization. *Electroanalysis* 14:1041–51
28. Maeda M, White HS, McClure DJ. 1986. Electrochemical behavior and surface structure of Pt thin film electrodes deposited on molecularly smooth mica. *J. Electroanal. Chem.* 200:383–87
29. Caston SL, McCarley RL. 2002. Characteristics of nanoscopic Au band electrodes. *J. Electroanal. Chem.* 529:124–34
30. Kim YT, Scarnulis DM, Ewing AG. 1986. Carbon-ring electrodes with 1-μm diameter. *Anal. Chem.* 58:1782–86
31. MacFarlane DR, Wong DKY. 1985. Thin-ring ultra-microelectrodes. *J. Electroanal. Chem.* 185:197–202
32. Macpherson JV, Jones CE, Unwin PR. 1998. Radial flow microring electrode: investigation of fast heterogeneous electron-transfer processes. *J. Phys. Chem. B* 102:9891–97
33. Lanyon YH, De Marzi G, Watson YE, Quinn AJ, Gleeson JP, et al. 2007. Fabrication of nanopore array electrodes by focused ion beam milling. *Anal. Chem.* 79:3048–55

34. Guerrette JP, Percival SJ, Zhang B. 2011. Voltammetric behavior of gold nanotrench electrodes. *Langmuir* 27:12218–25
35. Menke EJ, Thompson MA, Xiang C, Yang LC, Penner RM. 2006. Lithographically patterned nanowire electrodeposition. *Nat. Mater.* 5:914–19
36. Xiang CX, Kung SC, Taggart DK, Yang F, Thompson MA, et al. 2008. Lithographically patterned nanowire electrodeposition: a method for patterning electrically continuous metal nanowires on dielectrics. *Am. Chem. Soc. Nano* 2:1939–49
37. Rassaei L, Singh PS, Lemay SG. 2011. Lithography-based nanoelectrochemistry. *Anal. Chem.* 83:3974–80
38. Gates BD, Xu QB, Thalladi VR, Cao TB, Knickerbocker T, Whitesides GM. 2004. Shear patterning of microdominos: a new class of procedures for making micro- and nanostructures. *Angew. Chem. Int. Ed.* 43:2780–83
39. Dickey MD, Lipomi DJ, Bracher PJ, Whitesides GM. 2008. Electrically addressable parallel nanowires with 30 nm spacing from micromolding and nanoskiving. *Nano Lett.* 8:4568–73
40. Lipomi DJ, Martinez RV, Rioux RM, Cademartiri L, Reus WF, Whitesides GM. 2010. Survey of materials for nanoskiving and influence of the cutting process on the nanostructures produced. *Am. Chem. Soc. Appl. Mater. Interfaces* 2:2503–14
41. Dawson K, Strutwolf J, Rodgers KP, Herzog G, Arrigan DWM, et al. 2011. Single nanoskived nanowires for electrochemical applications. *Anal. Chem.* 83:5535–40
42. Cahill PS, Walker QD, Finnegan JM, Mickelson GE, Travis ER, Wightman RM. 1996. Microelectrodes for the measurement of catecholamines in biological systems. *Anal. Chem.* 68:3180–86
43. Li Y, Bergman D, Zhang B. 2009. Preparation and electrochemical response of 1–3 nm Pt disk electrodes. *Anal. Chem.* 81:5496–502
44. Sun P. 2010. Cylindrical nanopore electrode and its application to the study of electrochemical reaction in several hundred attoliter volume. *Anal. Chem.* 82:276–81
45. Velmurugan J, Sun P, Mirkin MV. 2009. Scanning electrochemical microscopy with gold nanotips: the effect of electrode material on electron transfer rates. *J. Phys. Chem. C* 113:459–64
46. Jena BK, Percival SJ, Zhang B. 2010. Au disk nanoelectrode by electrochemical deposition in a nanopore. *Anal. Chem.* 82:6737–43
47. Zhang B, Zhang YH, White HS. 2004. The nanopore electrode. *Anal. Chem.* 76:6229–38
48. Agyekum I, Nimley C, Yang CX, Sun P. 2010. Combination of scanning electron microscopy in the characterization of a nanometer-sized electrode and current fluctuation observed at a nanometer-sized electrode. *J. Phys. Chem. C* 114:14970–74
49. Sun Y, Liu YW, Liang ZX, Xiong L, Wang AL, Chen SL. 2009. On the applicability of conventional voltammetric theory to nanoscale electrochemical interfaces. *J. Phys. Chem. C* 113:9878–83
50. Liu YW, He R, Zhang QF, Chen SL. 2010. Theory of electrochemistry for nanometer-sized disk electrodes. *J. Phys. Chem. C* 114:10812–22
51. Liu Y, Zhang Q, Chen S. 2010. The voltammetric responses of nanometer-sized electrodes in weakly supported electrolyte: a theoretical study. *Electrochim. Acta* 55:8280–86
52. Gewirth AA, Craston DH, Bard AJ. 1989. Fabrication and characterization of microtips for scanning tunneling microscopy. *J. Electroanal. Chem.* 261:477–82
53. Nagahara LA, Thundat T, Lindsay SM. 1989. Preparation and characterization of STM tips for electrochemical studies. *Rev. Sci. Instrum.* 60:3128–30
54. Penner RM, Heben MJ, Lewis NS. 1989. Preparation and electrochemial characterization of conical and hemispherical ultramicroelectrodes. *Anal. Chem.* 61:1630–36
55. Sun P, Mirkin MV. 2008. Electrochemistry of individual molecules in zeptoliter volumes. *J. Am. Chem. Soc.* 130:8241–50
56. Zhang B, Zhang YH, White HS. 2006. Steady-state voltammetric response of the nanopore electrode. *Anal. Chem.* 78:477–83
57. Merkoci A. 2006. Carbon nanotubes in analytical sciences. *Microchim. Acta* 152:157–74
58. Merkoci A, Pumera M, Llopis X, Perez B, del Valle M, Alegret S. 2005. New materials for electrochemical sensing. VI. Carbon nanotubes. *Trends Anal. Chem.* 24:826–38

59. McCreery RL. 2008. Advanced carbon electrode materials for molecular electrochemistry. *Chem. Rev.* 108:2646–87
60. Yang WR, Ratinac KR, Ringer SP, Thordarson P, Gooding JJ, Braet F. 2010. Carbon nanomaterials in biosensors: Should you use nanotubes or graphene? *Angew. Chem. Int. Ed.* 49:2114–38
61. Novoselov KS, Geim AK, Morozov SV, Jiang D, Zhang Y, et al. 2004. Electric field effect in atomically thin carbon films. *Science* 306:666–69
62. Kong J, Soh HT, Cassell AM, Quate CF, Dai HJ. 1998. Synthesis of individual single-walled carbon nanotubes on patterned silicon wafers. *Nature* 395:878–81
63. Yang SL, Guo DY, Su L, Yu P, Li D, et al. 2009. A facile method for preparation of graphene film electrodes with tailor-made dimensions with Vaseline as the insulating binder. *Electrochem. Commun.* 11:1912–15
64. Li M, Xu S, Tang M, Liu L, Gao F, Wang YL. 2011. Direct electrochemistry of horseradish peroxidase on graphene-modified electrode for electrocatalytic reduction towards H_2O_2. *Electrochim. Acta* 56:1144–49
65. Shao YY, Wang J, Wu H, Liu J, Aksay IA, Lin YH. 2010. Graphene based electrochemical sensors and biosensors: a review. *Electroanalysis* 22:1027–36
66. Hu YJ, Jin JA, Zhang H, Wu P, Cai CX. 2010. Graphene: synthesis, functionalization and applications in chemistry. *Acta Phys. Chim. Sin.* 26:2073–86
67. Campbell JK, Sun L, Crooks RM. 1999. Electrochemistry using single carbon nanotubes. *J. Am. Chem. Soc.* 121:3779–80
68. Heller I, Kong J, Heering HA, Williams KA, Lemay SG, Dekker C. 2005. Individual single-walled carbon nanotubes as nanoelectrodes for electrochemistry. *Nano Lett.* 5:137–42
69. Heller I, Kong J, Williams KA, Dekker C, Lemay SG. 2006. Electrochemistry at single-walled carbon nanotubes: the role of band structure and quantum capacitance. *J. Am. Chem. Soc.* 128:7353–59
70. Day TM, Unwin PR, Wilson NR, Macpherson JV. 2005. Electrochemical templating of metal nanoparticles and nanowires on single-walled carbon nanotube networks. *J. Am. Chem. Soc.* 127:10639–47
71. Day TM, Unwin PR, Macpherson JV. 2007. Factors controlling the electrodeposition of metal nanoparticles on pristine single walled carbon nanotubes. *Nano Lett.* 7:51–57
72. Bertoncello P, Edgeworth JP, Macpherson JV, Unwin PR. 2007. Trace level cyclic voltammetry facilitated by single-walled carbon nanotube network electrodes. *J. Am. Chem. Soc.* 129:10982–83
73. Dumitrescu I, Dudin PV, Edgeworth JP, Macpherson JV, Unwin PR. 2010. Electron transfer kinetics at single-walled carbon nanotube electrodes using scanning electrochemical microscopy. *J. Phys. Chem. C* 114:2633–39
74. Adams KL, Puchades M, Ewing AG. 2008. In vitro electrochemistry of biological systems. *Annu. Rev. Anal. Chem.* 1:329–55
75. Wang W, Zhang SH, Li LM, Wang ZL, Cheng JK, Huang WH. 2009. Monitoring of vesicular exocytosis from single cells using micrometer- and nanometer-sized electrochemical sensors. *Anal. Bioanal. Chem.* 394:17–32
76. Huang WH, Pang DW, Tong H, Wang ZL, Cheng JK. 2001. A method for the fabrication of low-noise carbon fiber nanoelectrodes. *Anal. Chem.* 73:1048–52
77. Menon VP, Martin CR. 1995. Fabrication and evaluation of nanoelectrode ensembles. *Anal. Chem.* 67:1920–28
78. Krishnamoorthy K, Zoski CG. 2005. Fabrication of 3D gold nanoelectrode ensembles by chemical etching. *Anal. Chem.* 77:5068–71
79. Baker WS, Crooks RM. 1998. Independent geometrical and electrochemical characterization of arrays of nanometer-scale electrodes. *J. Phys. Chem. B* 102:10041–46
80. Sandison ME, Cooper JM. 2006. Nanofabrication of electrode arrays by electron-beam and nanoimprint lithographies. *Lab Chip* 6:1020–25
81. Hyde ME, Davies TJ, Compton RG. 2005. Fabrication of random assemblies of metal nanobands: a general method. *Angew. Chem. Int. Ed.* 44:6491–96
82. Compton RG, Wildgoose GG, Rees NV, Streeter I, Baron R. 2008. Design, fabrication, characterisation and application of nanoelectrode arrays. *Chem. Phys. Lett.* 459:1–17
83. Ueno K, Hayashida M, Ye JY, Misawa H. 2005. Fabrication and electrochemical characterization of interdigitated nanoelectrode arrays. *Electrochem. Commun.* 7:161–65

84. Nagase T, Gamo K, Kubota T, Mashiko S. 2006. Direct fabrication of nano-gap electrodes by focused ion beam etching. *Thin Solid Films* 499:279–84
85. Tu Y, Lin YH, Yantasee W, Ren ZF. 2005. Carbon nanotubes based nanoelectrode arrays: fabrication, evaluation, and application in voltammetric analysis. *Electroanalysis* 17:79–84
86. Tu Y, Lin YH, Ren ZF. 2003. Nanoelectrode arrays based on low site density aligned carbon nanotubes. *Nano Lett.* 3:107–9
87. Watkins JJ, White HS. 2004. The role of the electrical double layer and ion pairing on the electrochemical oxidation of hexachloroiridate(III) Pt electrodes of nanometer dimensions. *Langmuir* 20:5474–83
88. Zhang YH, Zhang B, White HS. 2006. Electrochemistry of nanopore electrodes in low ionic strength solutions. *J. Phys. Chem. B* 110:1768–74
89. Chen SL, Kucernak A. 2002. The voltammetric response of nanometer-sized carbon electrodes. *J. Phys. Chem. B* 106:9396–404
90. He R, Chen SL, Yang F, Wu BL. 2006. Dynamic diffuse double-layer model for the electrochemistry of nanometer-sized electrodes. *J. Phys. Chem. B* 110:3262–70
91. Dickinson EJF, Compton RG. 2009. Diffuse double layer at nanoelectrodes. *J. Phys. Chem. C* 113:17585–89
92. Hoeben FJM, Heller I, Albracht SPJ, Dekker C, Lemay SG, Heering HA. 2008. Polymyxin-coated Au and carbon nanotube electrodes for stable [NiFe]-hydrogenase film voltammetry. *Langmuir* 24:5925–31
93. Hoeben FJM, Meijer FS, Dekker C, Albracht SPJ, Heering HA, Lemay SG. 2008. Toward single-enzyme molecule electrochemistry: [NiFe]-hydrogenase protein film voltammetry at nanoelectrodes. *Am. Chem. Soc. Nano* 2:2497–504
94. Bard AJ. 2008. Toward single enzyme molecule electrochemistry. *Am. Chem. Soc. Nano* 2:2437–40
95. Guo J, Ho C-N, Sun P. 2011. Electrochemical studies of chemically modified nanometer-sized electrodes. *Electroanalysis* 23:481–86
96. Ye HC, Crooks RM. 2005. Electrocatalytic O_2 reduction at glassy carbon electrodes modified with dendrimer-encapsulated Pt nanoparticles. *J. Am. Chem. Soc.* 127:4930–34
97. Ye H, Crooks JA, Crooks RM. 2007. Effect of particle size on the kinetics of the electrocatalytic oxygen reduction reaction catalyzed by Pt dendrimer–encapsulated nanoparticles. *Langmuir* 23:11901–6
98. Kumar S, Zou SZ. 2009. Electrooxidation of CO on uniform arrays of Au nanoparticles: effects of particle size and interparticle spacing. *Langmuir* 25:574–81
99. Kwon SJ, Zhou H, Fan F-RF, Vorobyev V, Zhang B, Bard AJ. 2011. Stochastic electrochemistry with electrocatalytic nanoparticles at inert ultramicroelectrodes—theory and experiments. *Phys. Chem. Chem. Phys.* 13:5394–402
100. Xiao X, Bard AJ. 2007. Observing single nanoparticle collisions at an ultramicroelectrode by electrocatalytic amplification. *J. Am. Chem. Soc.* 129:9610–12
101. Xiao X, Fan F-RF, Zhou J, Bard AJ. 2008. Current transients in single nanoparticle collision events. *J. Am. Chem. Soc.* 130:16669–77
102. Kwon SJ, Fan F-RF, Bard AJ. 2010. Observing iridium oxide (IrO_x) single nanoparticle collisions at ultramicroelectrodes. *J. Am. Chem. Soc.* 132:13165–67
103. Bard AJ. 2010. Inner-sphere heterogeneous electrode reactions. Electrocatalysis and photocatalysis: the challenge. *J. Am. Chem. Soc.* 132:7559–67
104. Amemiya S, Bard AJ, Fan F-RF, Mirkin MV, Unwin PR. 2008. Scanning electrochemical microscopy. *Annu. Rev. Anal. Chem.* 1:95–131
105. Stoica L, Neugebauer S, Schuhmann W. 2008. Scanning electrochemical microscopy (SECM) as a tool in biosensor research. *Biosens. 21st Century* 109:455–92
106. Katemann BB, Schulte A, Schuhmann W. 2004. Constant-distance mode scanning electrochemical microscopy. Part II: High-resolution SECM imaging employing Pt nanoelectrodes as miniaturized scanning probes. *Electroanalysis* 16:60–65
107. Sanchez-Sanchez CM, Rodriguez-Lopez J, Bard AJ. 2008. Scanning electrochemical microscopy. 60. Quantitative calibration of the SECM substrate generation/tip collection mode and its use for the study of the oxygen reduction mechanism. *Anal. Chem.* 80:3254–60

108. Mezour MA, Cornut R, Hussien EM, Morin M, Mauzeroll J. 2010. Detection of hydrogen peroxide produced during the oxygen reduction reaction at self-assembled thiol-porphyrin monolayers on gold using SECM and nanoelectrodes. *Langmuir* 26:13000–6
109. Etienne M, Anderson EC, Evans SR, Schuhmann W, Fritsch I. 2006. Feedback-independent Pt nanoelectrodes for shear force–based constant-distance mode scanning electrochemical microscopy. *Anal. Chem.* 78:7317–24
110. Fan F-RF, Bard AJ. 1995. Electrochemical detection of single molecules. *Science* 267:871–74
111. Fan F-RF, Kwak J, Bard AJ. 1996. Single molecule electrochemistry. *J. Am. Chem. Soc.* 118:9669–75
112. Wightman RM. 2006. Probing cellular chemistry in biological systems with microelectrodes. *Science* 311:1570–74
113. Wu WZ, Huang WH, Wang W, Wang ZL, Cheng JK, et al. 2005. Monitoring dopamine release from single living vesicles with nanoelectrodes. *J. Am. Chem. Soc.* 127:8914–15
114. Cheng H, Huang WH, Chen RS, Wang ZL, Cheng JK. 2007. Carbon fiber nanoelectrodes applied to microchip electrophoresis amperometric detection of neurotransmitter dopamine in rat pheochromocytoma (PC12) cells. *Electrophoresis* 28:1579–86
115. Li Z-Y, Zhou W, Wu Z-X, Zhang R-Y, Xu T. 2009. Fabrication of size-controllable ultrasmall-disk electrode: monitoring single vesicle release kinetics at tiny structures with high spatio-temporal resolution. *Biosens. Bioelectron.* 24:1358–64

Annual Review of
Analytical Chemistry

Volume 5, 2012

Contents